

Physics REBoot Venezuela.  
Bootcamp # 3: Quantum Information Science & Technology.

**Quantum algorithms: *a very short introduction*** <sup>1</sup>

J. G. R. Sánchez Chávez  
*Universidad de los Andes.*

Miguel Luna  
*Universidad Católica Andrés Bello.*

Kevin Durán  
*Universidad de los Andes.*

Timothy Sandoval  
*Universidad de Carabobo.*

Barbara Montañes  
*Instituto Venezolano de Investigaciones Científicas.*

Sara González  
*Universidad Simón Bolívar.*

**Advisors:**  
Sarah Hagen  
*University of Illinois at Urbana-Champaign.*

Mauricio Gomez Vioria  
*Université Paris-Saclay.*

**Abstract**

We present a minimal introduction to quantum algorithms aimed at discussing the main aspects of their theoretical and experimental implementation in information processing and quantum computing. After introducing a brief analysis of algorithms as a calculation tool, we discuss the Deutsch-Jozsa and Shor's algorithms with their quantum mechanical implications, including a discussion of some implementations on real physical systems. Qubitization is introduced as a means to study spin 1/2 systems, with the aid of canonical commutation relations, and finally, the variational quantum eigensolver algorithm is presented.

---

<sup>1</sup>Project

# Contents

<b>1</b>	<b>Introduction</b>	<b>3</b>
<b>2</b>	<b>Deutsch–Jozsa algorithm</b>	<b>3</b>
2.1	Demonstrations of Deutsch-Jozsa . . . . .	4
<b>3</b>	<b>Shor’s algorithm</b>	<b>6</b>
<b>4</b>	<b>Quantum signal processing: <i>an overview</i></b>	<b>8</b>
<b>5</b>	<b>Qubitization</b>	<b>9</b>
5.1	Second quantization for fermions . . . . .	9
5.2	The Jordan-Wigner transformation . . . . .	11
<b>6</b>	<b>Variational quantum eigensolver (VQE) algorithm</b>	<b>12</b>

# 1 Introduction

The superior efficiency of quantum computation one may expect with respect to classical computation may be ascribed just to the system's quantum dynamical properties:

- Interference,
- Entanglement,
- and Von Neumann wave function reduction.

Beside the aforementioned concepts, classical information processing is inherently serial, while quantum information transmission is essentially parallel.

As it was implied in the Church-Turing thesis, to solve a computational problem faster, one may (1) reduce the time to implement a single step, (2) perform many steps in parallel, or (3) reduce the total number of steps to completion via the design of a clever algorithm. Since quantum computers violate the extended Church-Turing thesis, this opened the possibility of an entirely new way of solving computational problems quickly [8].

The power of quantum algorithms ultimately derives from the exponential complexity of quantum systems — the state of a system of  $n$  entangled qubits is described by (and can thus encode)  $N = 2^n$  complex coefficients, as discussed in the previous chapter. Moreover, the application of each elementary gate on, say, two qubits updates the  $2^n$  complex numbers describing the state, thereby seeming to perform  $2^n$  computations in a single step. On the other hand, at the end of the computation, when the  $n$  qubits are measured, the result is just  $n$  classical bits. The challenge of designing useful and advantageous quantum algorithms derives from the tension between these two phenomena — one must find tasks [8] whose operational solutions both make use of this parallelism and yield a final quantum state that has a high probability of returning valuable information upon measurement. Successful approaches take advantage of the phenomenon of quantum interference for generating useful results.

This project aims to discuss the main aspects of the theoretical and experimental implementation of quantum algorithms.

## 2 Deutsch–Jozsa algorithm

The algorithm consists of determining if a Boolean function is balanced (50 percent of the results are "0" and 50 percent of the results are "1") or constant (100 percent of the results are "0" or 100 percent of the results are "1"). A classical algorithm can solve the problem in at most  $2^{n-1} + 1$  iterations. In the worst case a constant function could be evaluated in half of the cases and still need a case to fully determine its nature.

The Deutsch-Jozsa algorithm takes advantage of the parallelism of the superposition of quantum states: in this algorithm there is a function (known as oracle)  $f(x_1, \dots, x_n)$  that takes  $n$  input

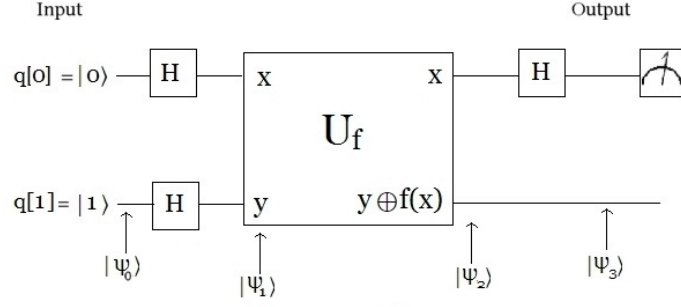


Figure 1: Deutsch-Jozsa algorithm quantum circuit. Source: [2]

bits and returns a binary value [2] (see also Fig. 1).

The purpose of this algorithm is to determine whether the function is constant or balanced by applying the input bits with the fewest possible number of iterations. The result will be the qubit  $|0\rangle$  if the function is constant (constructive interference) and the qubit  $|1\rangle$  if the function is balanced (destructive interference).

The application of several gates leads to a probability amplitude of some states that is function of the original unknown Boolean function:

$$\left| \frac{1}{2^n} \sum_{x=0}^{2^n-1} (-1)^{f(x)} \right|^2 \quad (2.1)$$

## 2.1 Demonstrations of Deutsch-Jozsa

Considering Fig. 1, let  $f(x)$  be a Boolean function that is either balanced or constant, as defined above. The algorithm starts with a control qubit in the state  $|0\rangle$  and the target qubit in the state  $|1\rangle$ . Then the state of the system is:

$$|\Psi_0\rangle = |0\rangle_c |1\rangle_t \quad (2.2)$$

Then one Hadamard gate is applied to each sub-system:

$$|\Psi_1\rangle = H |\Psi_0\rangle = H_c |0\rangle_c H_t |1\rangle_t = \frac{1}{2}(|0\rangle + |1\rangle)_c (|0\rangle - |1\rangle)_t \quad (2.3)$$

Then an "oracle" gate is applied to the resulting state with inputs  $|x\rangle, |y\rangle$  and output  $|x\rangle, |y \oplus f(x)\rangle$

$$|\Psi_2\rangle = U_f |\Psi_1\rangle = \frac{1}{2}(|0\rangle + |1\rangle)_c (|0 \oplus f(x)\rangle - |1 \oplus f(x)\rangle)_t \quad (2.4)$$

Looking closely, it is easy to note that if  $f(x) = 0$  then  $0 \oplus f(x) = 0$  and  $1 \oplus f(x) = 1$ , similarly if  $f(x) = 1$  then  $0 \oplus f(x) = 1$  and  $1 \oplus f(x) = 0$ , so by substitution it is possible to

write the equation as:

$$|\Psi_2\rangle = \frac{1}{2}(|0\rangle + |1\rangle)_c (|0 \oplus f(x)\rangle - |1 \oplus f(x)\rangle)_t = \frac{1}{2}(-1)^{f(0)}|0\rangle_c (|0\rangle - |1\rangle)_t + (-1)^{f(1)}|1\rangle_c (|0\rangle - |1\rangle)_t \quad (2.5)$$

Finally if the Hadamard gate is applied again on the control qubit, it leads to:

$$|\Psi_3\rangle = H_c |\Psi_2\rangle = \frac{1}{2}((-1)^{f(0)} H_c |0\rangle_c (|0\rangle - |1\rangle)_t + (-1)^{f(1)} H_c |1\rangle_c (|0\rangle - |1\rangle)_t) \quad (2.6)$$

$$\Rightarrow |\Psi_3\rangle = \frac{1}{2} \left( \left( \frac{(-1)^{f(0)} + (-1)^{f(1)}}{\sqrt{2}} \right) |0\rangle_c + \left( \frac{(-1)^{f(0)} - (-1)^{f(1)}}{\sqrt{2}} \right) |1\rangle_c \right) (|0\rangle - |1\rangle)_t \quad (2.7)$$

And here is possible to see that in the cases where  $f(0) = f(1)$ , the amplitude of qubit  $|1\rangle$  becomes 0 and the amplitude of  $|0\rangle$  is 1. In the case where  $f(0) \neq f(1)$  the amplitude of qubit  $|1\rangle$  becomes 1 and the amplitude of  $|0\rangle$  becomes 0. This means that a single measurement of the control qubit will express if the function is balanced or not.

The generalization to  $n$  control qubits is also possible and using a similar procedure one is able to obtain the following expression for the probability of a measurement projection in the base state  $|0^{\otimes n}\rangle_c$ :

$$\left| \frac{1}{2^n} \sum_{x=0}^{2^n-1} (-1)^{f(x)} \right|^2 \quad (2.8)$$

which means that if  $f(x_i) = f(x_j)$  measuring the base state will occur with the maximum probability (1) but if  $f(x_i) \neq f(x_j)$  this will occur with 0 probability.

The Deutsch–Jozsa algorithm has been realized experimentally, using bulk nuclear magnetic resonance techniques, employing nuclear spins as quantum bits.

In contrast, the ion trap processor utilizes the motional and electronic quantum states of individual atoms as qubits, and in principle is easier to scale to many qubits. Experimental advances in the latter area include the realization of a two-qubit quantum gate, the entanglement of four ions, quantum state engineering and entanglement-enhanced phase estimation.

Classically, this evaluation requires two function calls, and examination of all possible outcomes, whereas the Deutsch–Jozsa quantum algorithm allows us to obtain the desired information with a single evaluation of the unknown  $f$ . The circuit diagram shown in Fig. 1 describes the implementation of the Deutsch–Jozsa algorithm with basic quantum operations. The two qubits required for the Deutsch–Jozsa algorithm are encoded in the electronic state and in the phonon (vibrational quantum) number of the axial vibration mode of the single trapped ion. Qubit operations are realized by applying laser pulses on the ‘carrier’ or the ‘blue side band’ of the electric quadrupole transition.

### 3 Shor's algorithm

For the classical implementation of Shor's algorithm reported by Selke [7], the quantum part of Shor's Algorithm consists of a loop that terminates when a certain modular exponentiation equals one. If the value immediately output from a quantum operation does not produce this result, various related values are tried, such as multiples. If this too fails, the quantum operation may also be retried. A similar pattern of a loop preventing wrong computed values from exiting together by retrying the operation with, critically, a changed input parameter to the computation, also applies to the overall algorithm that includes the quantum part. Classical gates cannot take advantage of the parallelism of quantum operations.

Entanglement, one of the basic advantages of quantum computation and its influence on speed of the quantum systems is not yet fully understood. According to Lanyon [3] the superior efficiency of Shor's algorithm is attributed to the quantum Fourier transform (QFT), and since entanglement is considered a necessary resource for quantum computational speedup, one would expect that the QFT will induce it. It seems as though, for the purpose of quantum speedup, it suffices for the QFT to simply operate on a highly entangled register rather than generating entanglement by itself.

There have been demonstrations of entangling quantum-logic gates in a range of physical architectures, ranging from trapped ions, to superconducting circuits, to single photons.

Unlike the case of bipartite entanglement, multipartite entanglement of a register of  $q > 2$  qubits is not as well understood [4], partly because no analog of the Schmidt decomposition was found for multipartite systems.

Axiomatic considerations have provided a set of properties that entanglement measures should satisfy [4]. These properties include the requirement that any entanglement measure should vanish for product (or separable) states. It should be invariant under local unitary operations and should not increase as a result of any sequence of local operations supplemented only by classical communication between the parties (LOCC - local operations and classical communication). Quantities that satisfy these properties are called entanglement monotones. These properties provide useful guidelines in the search for entanglement measures for multipartite quantum states. Entanglement measures based on metric properties of the Hilbert space and on polynomial invariants were proposed and shown to satisfy these requirements.

In the case of Shor's algorithm, a superposition is built in the preprocessing stage, in a manner that does not make use of interference (modular exponentiation is performed on each computational basis state separately). This superposition in fact already contains the desired information (the period), and the QFT is merely needed to extract this information (by canceling the shift).

Therefore, it can be argued that the preprocessing stage is where quantum parallelism is

used, and the QFT introduces quantum interference. This claim is supported by the fact that the QFT does not increase the entanglement of the register.

As for the physical architectures for the implementation of Shor's algorithm, nuclear magnetic resonance (NMR) and photonic systems, there are some open questions in both cases [5]. In the only demonstration to date, a compiled set of gate operations were implemented in a liquid NMR architecture. It is difficult to prepare the qubits in pure states and control their coherent evolution. However, since the qubits are at all times in a highly mixed state, and the dynamics can be fully modelled classically, neither the entanglement nor the coherent control at the core of Shor's algorithm can be implemented or verified.

Additionally, photonic systems cannot be scaled to a larger number of qubits due to limitations of their size and stability. Nevertheless, a recent experimental demonstration of Shor's algorithm was obtained by means of optical waveguides integrated on silica-on-silicon chips. Even if the efficiency of the single-photon source and detectors still does not appear to be very good, the suggested architecture is promising for the implementation of large-scale quantum circuits on many qubits. Since the recent developments in nanostructure fabrication, today in both approaches the scalability is yet questionable [5].

Exploring the photonic system architecture deeper, according to Lanyon [3], photon polarisation experiences essentially zero decoherence in free space; uniquely, photonic gates have been fully characterised, produce the highest entanglement, and are the fastest of any architecture. The combination of long decoherence time and fast gate speeds make photonic architectures a promising approach for quantum computation, where large numbers of gates will need to be executed within the coherence lifetime of the qubits.

Demonstration of these processes is a necessary step on the path towards scalable quantum computing. These processes include the ability to generate entanglement between qubits by coherent application of a series of quantum gates: this represents a significant challenge to current technology.

The argument and function registers are bundles of  $n$  and  $m$  qubits; the nested order-finding structure uses  $U|y\rangle = |Cy \bmod N\rangle$ , where the initial function-register state is  $|y\rangle = 1$ . The algorithm is completed by a logical measurement of the argument register, and reversing the order of the argument qubits (see Fig. 2).

Experiments demonstrate the feasibility of executing complex, multiple-gate quantum circuits involving coherent multi-qubit super positions of data registers [3]. We present two different implementations of the order-finding routine at the heart of Shor's algorithm, characterizing the algorithmic and circuit performances.

Order-finding routines are a specific case of phase-estimation routines, which in turn underpin a wide variety of quantum algorithms, such as those in quantum chemistry. Besides providing

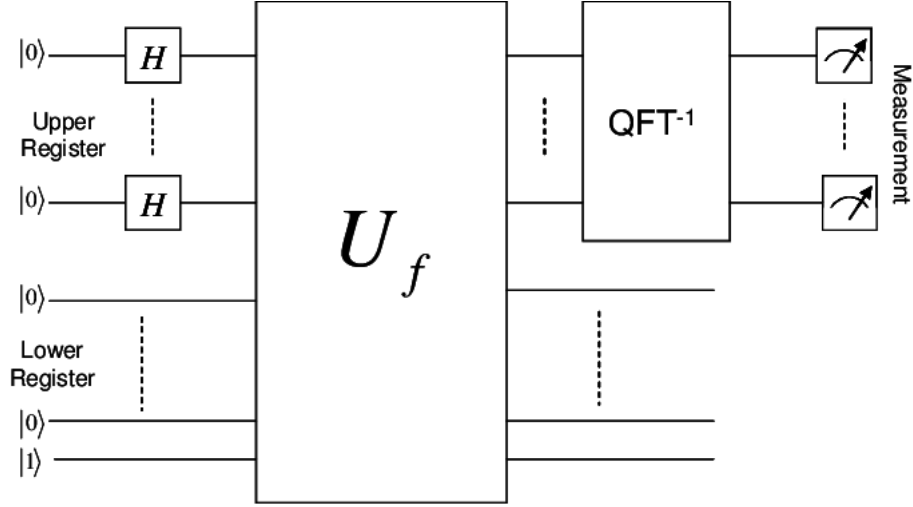


Figure 2: Shor's algorithm quantum circuit. Source: [3]

a proof of the use of quantum entanglement for arithmetic calculations, this work points to a number of interesting avenues for future research—in particular, the advantages of tailoring algorithm design to specific physical architectures, and the urgent need for efficient diagnostic methods of large quantum information circuits.

## 4 Quantum signal processing: *an overview*

Signal processing permits the optimal experimental signal to vector (qubit) correspondence [1].

Quantization, measurement and consistency in signal processing algorithms a general schematic comes as follows Instrument/Apparatus amplifier, processor, feature/characteristic generator, signal enhancement, feature (physical property) extraction/isolation, feature selection/dimensional reduction, feature translation: classification and post processing, control apparatus/instrument interface (lecture) and finally device controller.

Removing artifice from input signals. Enhances signal-to-noise ratio, the output is a signal with the same nature of the input (both states are in the temporal domain) then its possible to generates the feature vectors, a subset selection and dimensional reduction, feature classification into logical control signals, increase performance.

Measurement: A non linear (probabilistic) mapping described in terms of a set of measurable vectors  $\{|\psi_i\rangle, i \in \mathcal{I}\}$  that span measurement subspaces  $\{S_m \in H, m \in \mathcal{I}\}$   $\mathcal{I}$  an index set states lie in the measurement subspace  $S_m$ , measurement are described in terms of a set of projection operators which forms a complete set of commuting observables C.C.O.C (i.e. can be measured



simultaneously) measuring collapses (projects) the state of the system onto a state compatible with the measurement outcome.

Repeated measurement on a system yields the same outcome. Discreteness (quantization) of the outcome refers to determined states with known outcome and probability one, even if initially the system is not in one of these determinate states, whose probability are the inner product between the arbitrary state and the determinate one.

Several criteria involving minimizing the error in the detection problem as minimizing a given set of state vectors i.e (minimize the sum of the squared norms of the error vectors) and choosing the optimal set of orthogonal vectors, imposed by orthogonality or general inner product constraints on algorithms.

By an analysis of the equivalence between the quantum measurement and signal processing algorithm, since physical constraints lie in the inner nature of the observation process, the quantum signal processing design is ultimately restricted by the general inner product properties.

Interpreting a discrete set of measurements as function computing programs can lead to optimal algorithms to produce response functions, aimed for a fine/grained control over the experimental parameters of the physical system [6].

By using a unitary quantum oracle  $\hat{O}$  it is possible to describe a Hamiltonian  $\hat{H}$ , the complexity of which is proportional to the numbers of queries in  $\hat{O}$ . Therefore one of the main tasks is searching for a quantum circuit with minimal queries.

## 5 Qubitization

Qubitization is the translation of a particle problem into a two-level systems problem. For the study of qubitization, different types of transformations have been developed, where the best known is the Jordan-Wigner transformation, which translates a problem of electrons (fermions) into a problem of qubits. In this way, we can write an electronic Hamiltonian, transform it and simulate it directly on a quantum computer.

### 5.1 Second quantization for fermions

Dirac's second quantization formalism is a generalization of the study of a one particle state function, applied to a system that consists of a variable number of particles in which charge conservation law holds. Applied to systems consisting of an indefinite number of zero charge particles like photons of the radiant field.

Fermions are identical particles that comply with the Pauli exclusion principle, due to this, the occupation number can be 0 or 1. This characteristic is very important in order to connect a many body problem with a problem of qubits. Another characteristic of fermions (as opposed to bosons) is that they are antisymmetric (functions) - see Fig. 3.

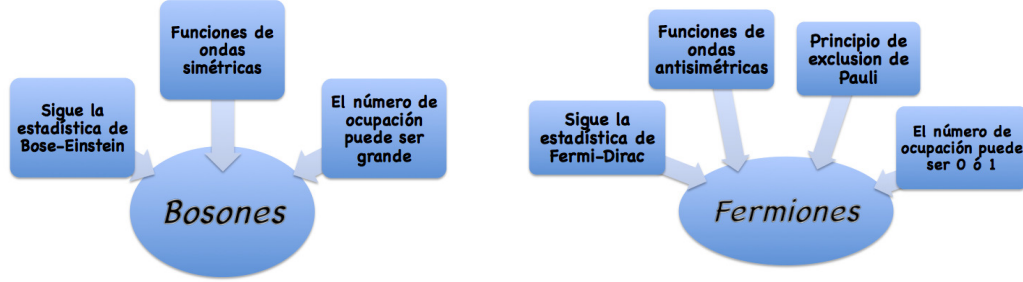


Figure 3: Description of bosons and fermions in Spanish. Source: Personal Collection.

The second quantization, also known as the occupation number representation, is a formalism used to describe and analyze quantum many-body systems. In this approach, many-body quantum states are represented on the basis of the Fock state, which is constructed by filling each single-particle state with a certain number of identical particles. The second quantization formalism introduces the creation and annihilation operators to build and handle Fock states, providing useful tools for the study of many-body quantum theory [9].

Due to the fermions are antisymmetric particles, we have that the creation and destruction operators must satisfy the following anticommutation relations:

$$\begin{aligned} \{\hat{a}_\alpha^\dagger, \hat{a}_\beta^\dagger\} &= 0, \quad \{\hat{a}_\alpha, \hat{a}_\beta\} = 0, \quad \{\hat{a}_\alpha, \hat{a}_\beta^\dagger\} = \delta_{\alpha\beta} \\ \hat{a}_\alpha \hat{a}_\beta &= 0, \quad \hat{a}_\alpha^\dagger \hat{a}_\beta^\dagger = 0 \end{aligned} \quad (5.1)$$

Creation operator generalize Fock space state functions, annihilation operator its complex conjugate quantity.

On the other hand, we have that the function of creation and destruct operations are given by

- **Creation operator  $\hat{a}_\alpha^\dagger$ :**

Must increment occupation number  $N_\alpha$  by one if  $N_\alpha = 0$ , and destroy the state if  $N_\alpha = 1$ . The creation operator is defined as:

$$\hat{a}_\alpha^\dagger |N_1, N_2, \dots, N_\alpha, \dots\rangle = (-1)^{S_\alpha} (1 - N_\alpha) |N_1, N_2, \dots, N_\alpha + 1, \dots\rangle \quad (5.2)$$

- **Annihilation operator  $\hat{a}_\alpha$ :**

It must decrement the occupation number  $N_\alpha$  by one if  $N_\alpha = 1$ , and destroy the state if

$N_\alpha = 0$ . The creation operator is defined as:

$$\hat{a}_\alpha |N_1, N_2, \dots, N_\alpha, \dots\rangle = (-1)^{S_\alpha} (N_\alpha) |N_1, N_2, \dots, N_\alpha - 1, \dots\rangle \quad (5.3)$$

Therefore,

$$\hat{N}_\alpha^2 = (\hat{a}_\alpha^\dagger \hat{a}_\alpha)^2 = \hat{a}_\alpha^\dagger \hat{a}_\alpha \hat{a}_\alpha^\dagger \hat{a}_\alpha = \hat{a}_\alpha^\dagger (1 - \hat{a}_\alpha \hat{a}_\alpha^\dagger) \hat{a}_\alpha = \hat{a}_\alpha^\dagger \hat{a}_\alpha = \hat{N}_\alpha \quad (5.4)$$

The field operators for fermions fulfill the following relations

$$\{\Psi_\sigma^\dagger(\vec{r}), \Psi_{\sigma'}^\dagger(\vec{r}')\} = \{\Psi_\sigma(\vec{r}), \Psi_{\sigma'}(\vec{r}')\} = 0 \quad (5.5)$$

and

$$\{\Psi_\sigma(\vec{r}), \Psi_{\sigma'}^\dagger(\vec{r}')\} = \delta_{\sigma\sigma'} \delta(\vec{r}, \vec{r}'). \quad (5.6)$$

## 5.2 The Jordan-Wigner transformation

The Jordan-Wigner transform (Fig.4) can be inverted, allowing us to express the Pauli operators in terms of the Fermionic operators  $a_1, \dots, a_n$ . In particular, we have

$$Z_j = a_j a_j^\dagger - a_j^\dagger a_j. \quad (5.7)$$

This observation may also be used to obtain an expression for  $X_j$  by noting that  $X_j = \sigma_j + \sigma_j^\dagger$ , and thus:

$$X_j = -(Z_1 \dots Z_{j-1})(a_j + a_j^\dagger) \quad (5.8)$$

Substituting in the expressions for  $Z_1, \dots, Z_{j-1}$  in terms of the Fermionic operators gives the desired expression for  $X_j$  in terms of the Fermionic operators. Similarly, we have

$$Y_j = i(Z_1 \dots Z_{j-1})(a_j - a_j^\dagger) \quad (5.9)$$

which, together with the expression for the  $Z_j$  operators, enables us to express  $Y_j$  solely in terms of the Fermionic operators.

Now it is possible to write a Hamiltonian for an electron system as:

$$H_e = \sum_{pq} h_{pq} \hat{a}_p^\dagger \hat{a}_q + \sum_{pqrs} g_{pq,rs} \hat{a}_p^\dagger \hat{a}_q^\dagger \hat{a}_r \hat{a}_s \quad (5.10)$$

with a state function:

$$|\Phi\rangle = \sum_{\pi} C_{\pi} |n_1, n_2, \dots, n_{N_o}\rangle, n_i = \{0, 1\} \quad (5.11)$$

The qubit counterpart of (5.10) and (5.11) are:

$$H_q = \sum_{i\alpha} h_i^{(\alpha)} \sigma_i^{(\alpha)} + \sum_{ij\alpha\beta} h_{ij}^{(\alpha\beta)} \sigma_i^{(\alpha)} \sigma_j^{(\beta)} + \dots \quad (5.12)$$

$$|\Phi\rangle = \sum_{\vec{\sigma}} C_{\vec{\sigma}} |\sigma_1^{(z)}, \sigma_2^{(z)}, \dots, \sigma_{N_a}^{(z)}\rangle, \sigma_k^{(z)} = \{\uparrow, \downarrow\}$$

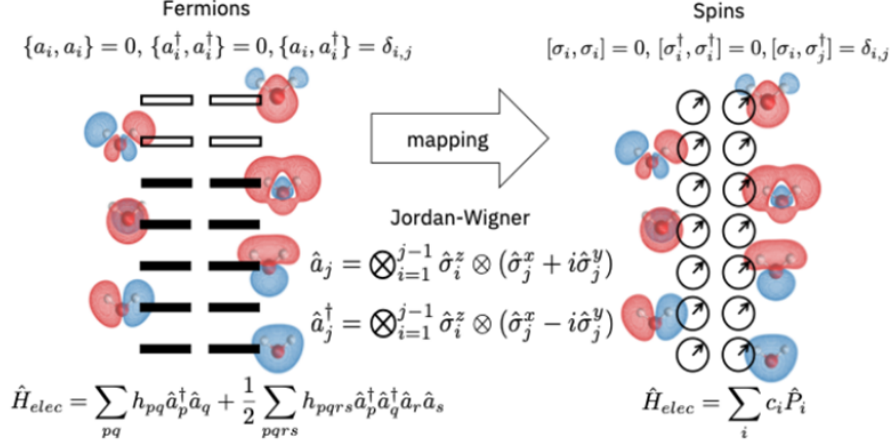


Figure 4: A picture describing Jordan Wigner mapping showing the equivalence between occupation number and spin representation of the spin-orbital state functions (depicted in the figure for a H<sub>2</sub>O molecule) [10].

## 6 Variational quantum eigensolver (VQE) algorithm

Electronic structure are a unique for different atom/molecular systems, and defines its physical and chemical properties. VQE is a hybrid method to get an accurate calculation of this physical feature, by using quantum and classical computational capabilities.

Main task to find a wave function for lower energy with the minimum number of parameters to vary using

$$E_0(\theta) = \frac{\langle \Psi_0 | U(\theta)^\dagger \hat{H}_{\text{tot}} U(\theta) | \Psi_0 \rangle}{\langle \Psi_0 | U(\theta)^\dagger U(\theta) | \Psi_0 \rangle} = E_{HF} + E_{corr} \quad (6.1)$$

By an accurate input (approximation state function of the atomic/molecular system) the algorithm is set to perform an optimization of the unitary transformations, that results in minimizing the energy, which splits in two parts. A quantum computer set up a quantum state function start vacuum state qubits, rotates qubits, entangle them obtaining the trial state function and finally measure it the results go to the classical computer, it finds new angles for the unitary rotations and gives a new state function, iterate the process to get lower eigenvalues and repeats this process until the solution converges and the algorithms stops.

The Hartree-Fock Hamiltonian for an electron system can be written in second quantization form as:

$$\begin{aligned}
 \hat{H}_e &= \sum_{pq} h_{pq} \hat{a}_p^\dagger \hat{a}_q + \sum_{pqrs} g_{pq,rs} \hat{a}_p^\dagger \hat{a}_q^\dagger \hat{a}_r \hat{a}_s \\
 h_{pq} &= \int \phi_p^*(r) \left( -\frac{1}{2} \nabla^2 - \sum_I \frac{Z_I}{R_I - r} \right) \phi_q(r) dr \\
 h_{pqrs} &= \int \frac{\phi_p^*(r_1) \phi_q^*(r_2) \phi_r(r_2) \phi_s(r_1)}{|r_1 - r_2|} dr_1 dr_2
 \end{aligned} \quad (6.2)$$

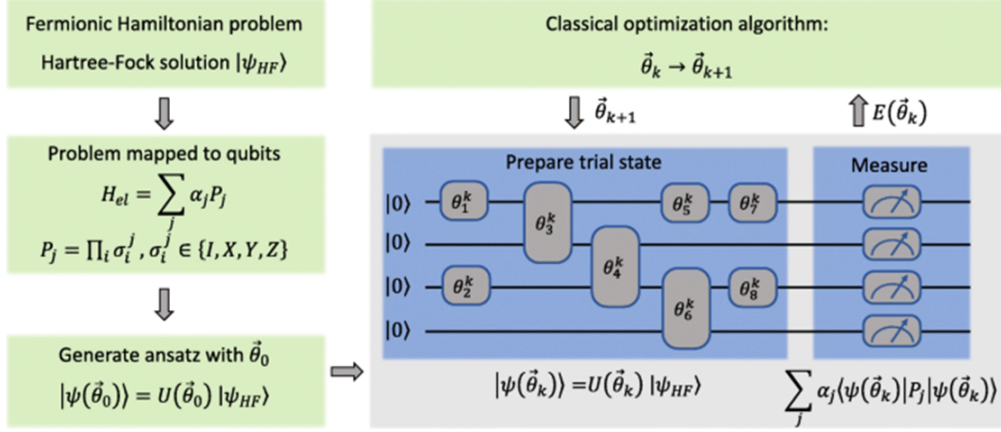


Figure 5: Variational quantum eigensolver scheme [11]

Hartree-Fock eigenvalues do not correspond to any real property of the ground state of the system, but calculations such as electron charge-density distributions and total energies of the system approximate real properties of the ground state.

Number of gates to represent unitary operators

$$\begin{aligned}
 U &= e^{itH} \approx \prod_j U_j^{(g)} \\
 U(\theta, T) &= U_1(\theta)U_2(T)
 \end{aligned} \tag{6.3}$$

Unitary transformations are not easy to find The entire Hamiltonian cannot be measured at once we need to separate it and measure all the parts. Hilbert qubit space is as big as the fock space, challenging to get the specific electronic states.

## References

- [1] Yonina C Eldar and Alan V Oppenheim. “Quantum signal processing”. In: *IEEE Signal Processing Magazine* 19.6 (2002), pp. 12–32.
- [2] Stephen Gulde et al. “Implementation of the Deutsch-Jozsa algorithm on an ion-trap quantum computer.” In: *Nature* 421 (2003), pp. 48–50. DOI: 10.1038/nature01336.
- [3] BP Lanyon et al. “Experimental demonstration of Shor’s algorithm with quantum entanglement”. In: *ArXiv* (2007).
- [4] Yonathan Most, Yishai Shimoni, and Biham Ofer. “Entanglement of periodic states, the quantum Fourier transform, and Shor’s factoring algorithm”. In: *The American Physical Society* 81 (2010), 052306-1 – 052306-8.
- [5] Buscemi Fabrizio. “Shor’s quantum algorithm using electrons in semiconductor nanostructures”. In: *The American Physical Society* 83 (2011).
- [6] Guang Hao Low and Isaac L Chuang. “Optimal Hamiltonian simulation by quantum signal processing”. In: *Physical review letters* 118.1 (2017), p. 010501.
- [7] David Selke. “A Classical Mechanism for Shor’s Algorithm Implementations”. In: *Applied Physics Research* 10 (2018), pp. 24–25.
- [8] Engineering National Academies of Sciences and Medicine. *Quantum Computing: Progress and Prospects*. Ed. by Emily Grumbling and Mark Horowitz. Washington, DC: The National Academies Press, 2019. ISBN: 978-0-309-47969-1. DOI: 10.17226/25196.
- [9] *Second Quantization*. [https://hmgong.es/wiki/Second\\\_quantization](https://hmgong.es/wiki/Second\_quantization).
- [10] *VQE algorithm for electronic structure calculation*. URL: [https://qiskit.org/documentation/nature/tutorials/01\\_electronic\\_structure.html](https://qiskit.org/documentation/nature/tutorials/01_electronic_structure.html).
- [11] *VQE diagram*. URL: [https://media.springernature.com/lw685/springer-static/image/art%3A10.1186%2Fs41313-021-00032-6/MediaObjects/41313\\_2021\\_32\\_Fig1\\_HTML.png](https://media.springernature.com/lw685/springer-static/image/art%3A10.1186%2Fs41313-021-00032-6/MediaObjects/41313_2021_32_Fig1_HTML.png).